

BEAM PARAMETER OPTIMIZATION FOR THE PHASE-I STAGE OF THE SPring-8 COMPACT SASE SOURCE (SCSS) PROJECT

Yujong Kim*, T. Shintake, H. Matsumoto, and H. Kitamura, RIKEN, SPring-8, Japan
 K. Sawada, Sumitomo Heavy Industries Ltd, Japan

Abstract

In April 2001, the SPring-8 Compact SASE Source (SCSS) project was launched to generate the soft X-ray. During the Phase-I stage of the SCSS project, the SASE-FEL source will generate 40 nm wavelength radiation with 230 MeV electron beam. To saturate the SASE mode within 20 m long in-vacuum undulator, the high quality electron beam should be supplied. In this paper, we have described the beam parameter optimization process from the injector to the bunch compressor to supply the required high quality beam at the Phase-I stage of the SCSS project.

1 INTRODUCTION

The SPring-8 Compact SASE Source (SCSS) is one of the fourth generation light source facility which is the linear accelerator based SASE-FEL [1]. Since the SCSS uses the high gradient C-band linear accelerator and the in-vacuum short period undulator, all facility will be compactly installed within 100 m length. By the end of 2007, we will install four units of the C-band main linear accelerator to generate 1 GeV electron beam, from which about six orders of magnitude brighter radiation than the current brightest third generation light source will be generated in the range of from 3 nm to 20 nm wavelength. The full description on the SCSS project can be found in the reference [1]. During the Phase-I stage from 2001 to 2005, we will install the injector, one C-band main linear accelerator and one bunch compressor (BC) to generate 230 MeV electron beam. In this paper, we will describe the beam parameter optimization process from the injector down to the bunch compressor to supply the required electron beam at the Phase-I stage of the SCSS project.

2 INJECTOR OPTIMIZATION

We have used ASTRA, PARMELA, POISSON, and SUPERFISH codes for the injector optimization. The beam-line layout and design beam parameters of the Phase-I stage of SCSS project is shown in Fig. 1. Confirmed parameters by the computer simulation as well as design parameters are also summarized in Table 1, where E is the beam energy, ϵ_{ns} (ϵ_n) is the transverse normalized rms slice (projected) emittance, σ_{δ_s} (σ_δ) is the rms relative slice (projected) energy spread, Q is the single bunch charge, $\Delta\tau$ (Δz) is the bunch length (FWHM), I_{pk} is the peak current. Here, all parameters are values at the exit positions of those elements. If there is only one value in a column, that

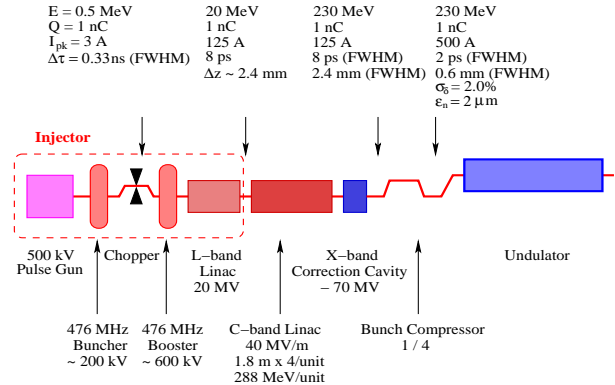


Figure 1: Beamline layout of the Phase-I stage of the SCSS.

Table 1: Parameters of the Phase-I stage of the SCSS.

Parameter	Gun	L-band	C-band	X-band	BC
E , MeV	0.5	20	300	230	230
ϵ_{ns} , μm	0.4	1.4	1.5	1.5	1.5
ϵ_n , μm	0.4	1.4	1.5	1.5	2.0/2.4
σ_{δ_s} , %	0.0	0.3	0.4	0.5	0.5
σ_δ , %	0.0	1.0	1.7	2.0	2.0
Q , nC	900	1	1	1	1
$\Delta\tau$, ps	3×10^5	8/16	8	8	2
Δz , mm	.	2.4/4.8	2.4	2.4	0.6
I_{pk} , A	3.0	125/62.5	125	125	500

means the confirmed parameter and the design parameter are same. When the confirmed value is different from the design value, the left means the design value, and the right means the confirmed value. Since electrons being apart further than one slippage length ($\sim \mu\text{m}$) will not interact with each other, we should focus the slice parameters to predict FEL performance [2]. Note the realistic slice values are much smaller than the given values in Table 1 because the current simulation codes overestimate the slice parameters.

The SCSS injector is consist of the 500 kV pulse gun with the CeB_6 single crystal cathode, 476 MHz buncher and booster cavities, and finally, 1428 MHz standing wave linac [1]. When the electron beam goes through the RF cavity, the projected emittance is diluted due to the time dependent fringe fields at the cavity entrance and exit regions. The dilution can be reduced by choosing the low RF frequencies of cavities and linac, by adjusting the average axial electric field at those regions, and by keeping small beam size [1], [3].

The buncher generates 200 kV energy modulation which induces the velocity modulation for the drift bunching. At the drift space between the buncher and the booster, where

* yjkim@spring8.or.jp

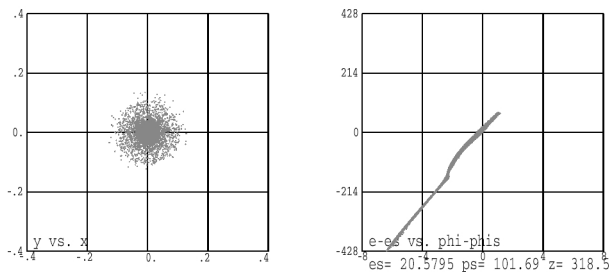


Figure 2: PARMELA simulation result after the L-band linac: (left) transverse beam profile, x [cm] versus y [cm] and (right) longitudinal phase space distribution, $\Delta\phi$ [degree] versus ΔE [keV].

the bunch length is compressed by the combined action of the buncher and the drift space, the space charge force is strong if the bunch charge is high. The space charge force and the emittance dilution in the drift space can be controlled by chopping the electron beam right after the buncher. Then, the electron beam is strongly focused by the first and second double Einzel lens to keep the beam size within 3 mm until the booster. By the help of the chopper, we select only the high quality beam with $\Delta\tau = 0.333$ ns, $Q = 1$ nC, and $\epsilon_{n,s} = \epsilon_n = 0.6$ μm .

According to the estimation result, where the space charge force is ignored, about 0.85 m drift space after the buncher is required to compress the bunch length from 0.333 ns to 16 ps [3]. However, the space charge force becomes strong before the beam goes through 0.85 m downstream as the bunch length is compressed. The transverse beam spreading due to the space charge force can be reduced to eight times smaller by increasing the beam energy to 1 MeV with the booster, which is located at 0.6 m downstream from the buncher [1]. [3]. Right after booster, we have applied the strong focusing by the third double Einzel lens to keep the beam size within 1.2 mm at the entrance of the L-band linac. After drifting 0.48 m long from the booster, the electron beam is compressed to 16 ps.

Our L-band standing wave linac is consist of $\pi/2$ mode eleven cells. Inside of the standing wave linac, the transverse beam size can be effectively reduced by the ponderomotive focusing force [4]. The PARMELA simulation result after the SCSS injector is shown in Fig. 2 where a small nonlinearity due to the space charge force and the RF curvature of the L-band linac is observed at the center of the bunch. The current optimized beam parameters after the SCSS injector is summarized in Table 1.

3 BUNCH COMPRESSOR

To saturate the SASE-FEL within 20 m long undulator, we need 500 A peak current or higher. Since the peak current is inversely proportional to the bunch length, we should compress the bunch length to obtain the peak current because no present injector technology can directly supply such a high peak current with low emittance. Bunch

compression can be obtained by rotating the bunch in the longitudinal phase space with the combined action of the RF precompressor linac and the magnetic chicane. The RF precompressor linac supplies the energy spread for the bunch rotation by the energy chirping, and the magnetic chicane supplies the nonzero dispersion region. When an electron with large energy spread goes through the nonzero dispersion region, its traveling path length is changed according to its energy [2], [5]. The bunch compressor operation is limited by two main sources. One is the coherent synchrotron radiation (CSR), and the other is the nonlinearity in the longitudinal phase space distribution.

When the bunch length is compressed in the bunch compressor, the bunch length may be much smaller than the radiation wavelength. In this case, the CSR can be generated. Since the CSR from tail electrons can overtake head electrons after the overtaking length, head electrons will be accelerated by the CSR, and tail electrons will be decelerated due to their own CSR loss. The electrons will be transversely kicked at the nonzero dispersion region due to the CSR induced correlated energy spread along the bunch. Note the projection emittance can be diluted due to the CSR in the bunch compressor while the slice emittance dilution is small enough.

Although the projected emittance dilution due to the CSR can be reduced by the symmetric double-chicane, the CSR induced microbunching instability in the chicane becomes strong when the initial uncorrelated energy spread and the emittance are small enough [2]. And though the microbunching instability can be cured by the wiggler combined single chicane, the slice emittance can be diluted due to the spontaneous radiation in the wiggler [2]. Therefore, we have chosen the normal single chicane for our bunch compressor by choosing somewhat large initial energy spread, the small bending angle, and somewhat large drift space between the first and second dipoles to control the CSR and the microbunching instability.

Optimized parameters of the SCSS bunch compressor is summarized in Table 2 where the emittance is the rms normalized value, and the energy spread is the rms value. Although our maximum R_{56} is about 100 mm which can be obtained by increasing the bending angle up to 0.14 radian, the normal operation parameters with $R_{56} = 24.8$ mm are displayed in Table 2. Note though the normal operational R_{56} can be reduced further by choosing higher σ_δ , we have chosen $\sigma_\delta = 2\%$ after considering the possible emittance dilution due to the misalignment and chromaticity. The layout of the SCSS bunch compressor is shown in Fig. 3. We have used ELEGANT, TraFiC4, and PARAO codes for this bunch compressor optimization.

The current optimized beam parameters after the bunch compressor for $R_{56} = 24.8$ mm case are summarized in Table 1. The peak current after bunch compressor is about 500 A as shown in Fig. 4(left). Since the energy change due to the CSR is small enough as shown in Fig. 4(right), the change of the rms relative projected energy spread $\Delta\sigma_\delta$ is about 0.012% after the bunch compressor [5]. Our real-

Table 2: Parameters of the SCSS bunch compressor.

Parameter	Unit	Value
beam energy E	MeV	230
initial bunch length Δz_i	mm	2.4
final bunch length Δz_f	mm	0.6
initial relative projected energy spread σ_δ	%	2.0
initial uncorrelated relative energy spread $\sigma_{\delta u}$	10^{-5}	~ 1
initial max relative energy deviation $(dE/E)_i$	10^{-2}	3.6
beam phase at the C-band linac ϕ_c	deg	11
momentum compaction factor R_{56}	mm	24.8
second order momentum compaction $ T_{566} $	mm	37.2
effective dipole length L_B	m	0.2
drift length between first and second dipoles ΔL	m	2.3
bending angle of each dipole θ_B	rad	0.07
magnetic field of each dipole $ B $	T	0.27
maximum horizontal dispersion η_{max}	m	0.18
maximum horizontal shift Δh	m	0.18
change of slice emittance $\Delta\epsilon_{r,s}$	%	~ 0
change of projected emittance $\Delta\epsilon_r$	%	60.0
change of σ_δ due to the CSR $\Delta\sigma_\delta$	%	0.012

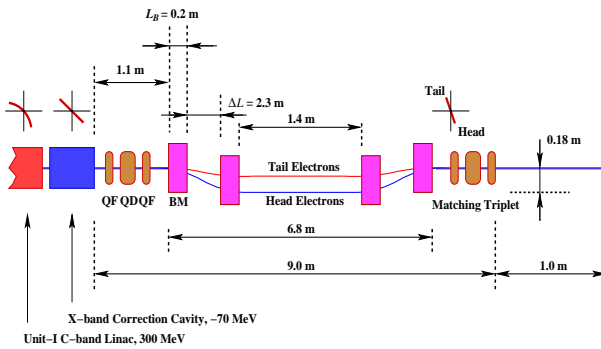


Figure 3: Layout of the SCSS bunch compressor.

istic projected emittance may be near $2 \mu\text{m}$ because the 1-D code ELEGANT overestimates the projected emittance growth due to the CSR [2]. Now, we are under cross-checking this value by the 3-D code TraFiC4.

Full bunch compression can be limited by the various nonlinearities due to the RF curvature, the space charge force, and wakefields. Since the beam energy is high enough at the SCSS BC, the space charge force can be ignorable. However, the nonlinearity due to the RF curvature

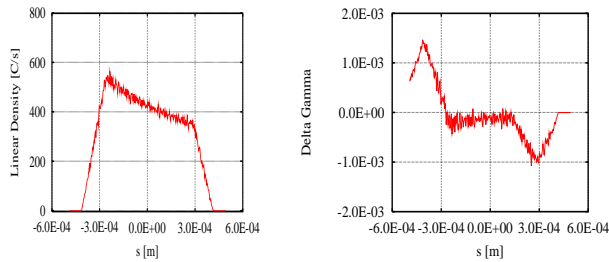


Figure 4: ELEGANT simulation results at the end region of the fourth dipole for $R_{56} = 24.8 \text{ mm}$ case: (left) linear density and (right) energy change due to CSR. Here, the negative s means the bunch head where the electrons are accelerated due to the CSR.

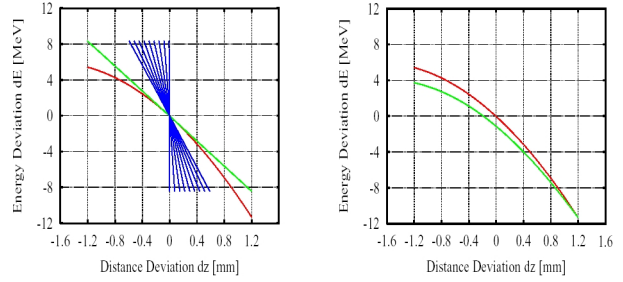


Figure 5: PARAO simulation results of the longitudinal phase space distribution when the beam phase at the C-band linac is 11 degree: (left) red - after C-band linac, green - after X-band correction cavity, blue - after the bunch compressor for $R_{56} = 16.8 \sim 32.8 \text{ mm}$ with 2.0 mm step conditions and (right) red - after C-band linac without the beam loading consideration, green - after C-band linac with the beam loading consideration.

of the C-band linac is strong when the beam center is located at 11 degree off from the RF crest. This type nonlinearity can be compensated by installing the X-band correction cavity between the precompressor linac and the bunch compressor as shown in Fig. 5(left) [2], [5]. Note though the linear energy distribution along the bunch is obtained, the beam is decelerated about 70 MeV due to the X-band correction cavity [2], [5]. If the CSR is ignored, the bunch length can be freely adjusted under the linearization condition by changing R_{56} as shown in Fig. 5(left). When the bunch length is short enough, the beam loading effect due to the longitudinal short range wakefields in the precompressor linac may compensate the nonlinearity due to the RF curvature. However, in our case, the beam loading in the C-band linac is not enough to compensate the nonlinearity under $\sigma_\delta \sim 2\%$ condition as shown in Fig. 5(right). Therefore, the higher harmonic correction cavity is essential for the proper bunch compressor operation.

4 SUMMARY

Although the design bunch length of 8 ps after injector is not obtained yet, the bunch length can be obtained by increasing the drift space for the drift bunching under the higher booster energy to control the space charge force. All slice parameters after the bunch compressor are within our design beam parameter range.

5 REFERENCES

- [1] T. Shintake *et al.*, in *Proc. the SPIE2001*, USA, to be published; <http://www-xfel.spring8.or.jp/Publication.htm>.
- [2] LCLS Conceptual Design Report, SLAC-R-593, 2002.
- [3] A. Wu Chao and M. Tigner, *Handbook of Accelerator Physics and Engineering*, (World Scientific, Singapore, 1998), p. 99.
- [4] J. Rosenzweig and L. Serafini, *Phys. Rev. E* **49**, 1599 (1994).
- [5] Yujong Kim, *et al.*, in *Proc. 24th ICF workshop*, Japan, to be published; <http://www-xfel.spring8.or.jp/Presentation.htm>.